Check for updates

Flexible hybrid film of polypyrrole incorporated chitosan as a biomimetic multistep electrochemical sensor of working temperature: a potentiodynamic study

Aranhikundan Shabeeba, [ID] Madari Palliyalil Sidheekha, [ID] Lijin Rajan and Yahya A. Ismail [ID] *

A polypyrrole/hydrogel hybrid film composed of macromolecular electrochemical machines fabricated through an *in situ* chemical polymerization of pyrrole is considered here as a flexible model material of the intracellular matrix of ectothermic muscle cells which is aware of ambient thermal energy. The polypyrrole component imparts excellent electroactivity and good electronic conductivity for the hybrid film. The hybrid film can go through *n* consecutive fundamental conformational energetic states progressively and reversibly under electrochemical control and acts as a multi-step macromolecular motor. Under constant electrochemical stimulus (cyclic voltammetry), increasing available thermal energy promotes deeper conformational movements of the polymeric chains due to the cooperative actuation of the constitutive electrochemical machines leading to the exchange of greater amounts of counterions and solvent for charge compensation and osmotic balance. The closed coulovoltammetric responses of the hybrid film guarantee the reversible nature of the polypyrrole redox reactions and reveal the absence of simultaneous irreversible reactions taking place in the studied potential window. At any reaction time, the extension of the reaction defined by the coulovoltammetric charge varies as a semilogarithmic function of the inverse of the temperature and acts as a self-sensor of reaction thermal conditions (reaction self-awareness). The results offer the potential for biomimetic sensing motors (intelligent devices) based on a polypyrrole/chitosan hybrid film imitating biological functions in which the driving and sensing signals can be read at any time during the reaction, through the same two connecting wires.

Introduction

A biological cell is a complex chemical reactor and the biochemical reactions (macromolecular motors) driving the cooperative conformational movements (cooperative actuation) of the reacting polymeric chains, changes of the intra and intermolecular interactions in the ambient dense biological gel, ionic exchanges and solvent exchanges cannot be described by the existing chemical models.[1–3] In ectothermic (cold-blooded) species, the environmental thermal conditions have significant effects on the muscular reactions.[4–6] At any instant, the reactions driving the conformational movements of the molecular motors from natural muscles are aware of the environmental temperature and temperature variations.[7] Natural muscles are electro-chemo-mechanical and thermo-mechanical transducers, respond to the reaction energy at various thermal conditions and send sensing signals regarding the working

thermal (chemical and physical) conditions to the brain through sensory neurons. But the origin of the reaction self-awareness and temperature-based efficiency gains is unknown. The best way to design such motors is to use conducting polymers as a base material that mimics the intracellular matrix (ICM) of the ectothermic muscle cell in its simplest form (one reactive macromolecule, one anion, and one solvent) during electrochemical reactions through the same two connecting wires.[8,9] The materials composition of conducting polymers (polymer/ion/solvent) can be tuned under electrochemical control through infinitesimal steps along a wide range, and different composition-dependent properties (stored conformational energy, stored counterions, stored charge, color, conductivity, volume, porosity, wettability, *etc.*) will be shifted during the redox reactions. These composition-dependent properties of conducting polymers mimic parallel reactions that occur in biological organs. The benzenoid/quinoid structures of the polymer change during the electrochemical reaction and allow/hinder monomeric rotations resulting in conformational movements which generate or

Advanced Materials Research Center, Department of Chemistry, University of Calicut, Thenhipalam, Kerala 673635, India. E-mail: aiyahya@uoc.ac.in

destroy free volume to accommodate or expel counterions and solvent for charge and osmotic balance: the polymer swells by oxidation and shrinks by reduction. These intra and inter-molecular interactions give rise to reversible molecular motors in solution.

Conducting polymers consisting of macromolecular electrochemical machines undergo oxidation/reduction reactions driving reversible structural changes and cooperative conformational movements (cooperative actuation) with the exchange of ions and solvent molecules with the surroundings.[10,11] Under electrochemical control, they can go through n consecutive chemical equilibrium steps or n consecutive fundamental conformational energetic states progressively and reversibly and act as a multi-step macromolecular motor.[12–14] The charge consumed (electrical energy or material potential evolution) by the reacting multi-step molecular motors involving electrochemically induced conformational movements of the macromolecular reactants senses or adapts instantaneously to the working thermal, chemical or mechanical perturbations at any moment in the reaction, through the same two connectivity.[15–19] That is, they replicate the events taking place inside the sarcomere.[20]

Among the various conductive polymers, polypyrrole (PPy) has attracted tremendous attention in various fields of electrical and electronic research owing to its high conductivity, light weight, facile synthesis, low operational voltage and biocompatibility.[21–30] The extensive application of conducting polymers is limited because of their fragile structure, brittleness, poor processability and poor mechanical strength, which can be compensated for through the fabrication of hybrid structures with hydrogels.[31,32] Chitosan (CS) is a naturally abundant hydrogel with a flexible backbone, and has received considerable attention as a prominent material for constructing different kinds of intelligent materials due to its structural and functional characteristics (for example a wide range of stimuli-responsive behavior, non-toxicity, biocompatibility, hydrophilicity, mechanical stability and high-quality adhesion).[33–35] The incorporation of a conducting polymer into a hydrogel synergizes the advantageous features of two relatively low-cost materials to obtain good conductivity, electroactivity (from the conducting polymer), good processability and mechanical strength (from the hydrogels).[36–42] This work is designed to investigate the influence of the experimental thermal conditions on the reversible redox reactions (reaction extension) of a flexible polypyrrole/chitosan hybrid film fabricated through *in situ* chemical polymerization of pyrrole on a chitosan film using cyclic voltammetry, with particular emphasis on the reproducibility of the electroactivity. The attained results could describe how the muscular reactions of cold-blooded beings occur and are aware of the working thermal conditions.

Experimental

Materials

Distilled pyrrole (Spectrochem, 99%) stored below 5 °C was used. Chitosan (MW = 190 000–31 0000, Sigma Aldrich Chemicals, 75% deacetylated), sodium chloride (Merck, 99.5%), ferric chloride (Merck, 98%), acetic acid (Spectrochem, 99.8%), methanol (Merck, 99%) and ethanol were used without further treatment. The solutions for use were prepared using double distilled water.

Fabrication of a polypyrrole/chitosan hybrid film

The fabrication of the polypyrrole/chitosan (PPy/CS) hybrid film was carried out by *in situ* chemical polymerization of pyrrole in an aqueous medium using ferric chloride as a catalyst. The procedure adapted for the fabrication of a hybrid film is same as described in previous studies.[36,43] This strategy is advantageous for the fabrication of flexible conducting polymer/hydrogel
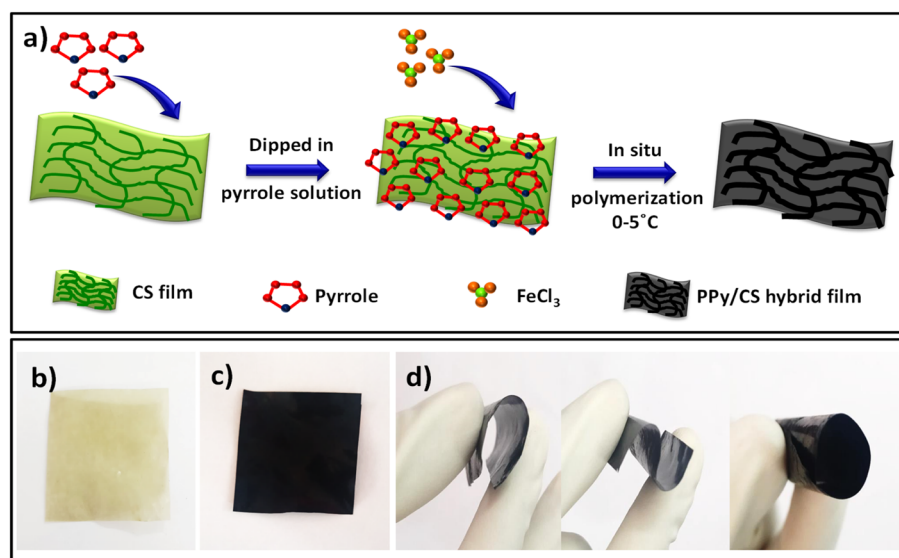

Fig. 1 (a) Schematic diagram of the fabrication of the PPy/CS hybrid film. Photographs of (b) the CS film, (c) the fabricated PPy/CS hybrid film. (d) Photographs of the PPy/CS hybrid film, revealing its flexibility.

hybrid films that can be used as good electrode materials in electrochemical applications. A schematic illustration of the fabrication of the PPy/CS hybrid film is shown in Fig. 1(a).

Characterization

A JASCO FTIR 4700 spectrometer with smart orbit accessories (ATR technology) was used to record the FTIR spectra of the films in a wavenumber range of 600 to 3600 cm^{-1}. Electrical conductivity measurements were carried out using a broadband dielectric spectrometer (Novocontrol Technologies, Germany) in a wide frequency window [10^{-2} to 10^{7} Hz] at room temperature and ambient pressure by placing the films between a couple of gold-plated parallel copper electrodes. The surface morphology of the films was examined using a field emission scanning electron microscope (ZEISS GeminiSEM 300) at an accelerating voltage of 5 kV. Elemental analysis was also carried out by employing an energy dispersive X-ray spectral attachment with SEM using a Gemini 300/EDS. For exploring the thermal behavior of the hybrid film, thermogravimetric analysis (TGA) was carried out at a heating rate of 10 °C min^{-1} from 30 to 650 °C employing a TA Q50 instrument under a nitrogen atmosphere. A universal test frame machine (Shimadzu AGX-PLUS-10 kN) was employed to study the mechanical characteristics of the hybrid film.

The electrochemical performance of the hybrid film was analyzed using a galvanostat–potentiostat workstation (Zahner Zennium Pro electrochemical analyzer) operating with computer controlled Thales XT analysis software. The analysis was carried out in a conventional three-electrode single compartment cell with the PPy/CS hybrid film, Ag/AgCl (3 M KCl) and Pt wire as the working electrode, reference electrode and counter electrode, respectively, and employing aqueous NaCl (1 M) as the electrolyte. The working electrode was fabricated by attaching the hybrid film (1 cm length and 0.2 cm width) to a platinum wire using conductive carbon paste. The hybrid films were used for electrochemical studies after one month of fabrication. The hybrid film was subjected to cyclic voltammetric (CV) cycles between −0.85 and 0.55 V in 1 M NaCl solution at a scan rate of 10 mV s^{-1}. Prior to the application of electrical signals, the film was allowed to equilibrate in the electrolyte. To gain further insight into the fundamental electrochemical behavior of the hybrid film, electrochemical impedance spectroscopy (EIS) was conducted in a frequency range of 0.1 Hz to 100 kHz at an open-circuit voltage of 10 mV. The influence of temperature (available thermal energy) on the redox charge (reaction extension) of the electrochemical reactions of the hybrid film was studied using consecutive potential cycles at different temperatures (ranging from 10 °C to 50 °C) under constant chemical (electrolyte concentration), physical (potential limit and scan rate) and mechanical (pressure) conditions using a thermostat. The reproducibility of the electrochemical activity of the hybrid film was analyzed using a control solution (1 M NaCl aqueous solution at 25 °C) by the following steps:

(a) The hybrid film electrode was dipped in a cell containing the voltammetric control solution (1 M NaCl aqueous solution at 25 °C) and the stationary CV responses were recorded.

(b) After the voltammetric control, the hybrid film electrode was dipped in another cell and placed in a thermostat with 1 M NaCl aqueous solution at 10 °C. The stationary CV responses were recorded under similar conditions.

(c) Then the electrode was placed back in the control solution and subjected to stationary voltammetric cycles.

Procedures (b) and (c) were repeated for various cell temperatures, which first increased (10 °C to 50 °C) and then decreased (50 °C to 10 °C).

Results and discussion

During the fabrication, when the CS film was suspended in the monomer solution, many pyrrole molecules were self-assembled along the chain of the chitosan owing to the strong hydrogen bonding interaction between the C=O group of chitosan and the NH group of pyrrole. This interaction is found to be stable. Through the subsequent *in situ* chemical polymerization, the CS film was gradually transformed from pale yellow to black, suggesting the coating of PPy on the CS film. Photographs of the pure CS film and PPy/CS hybrid film are shown in Fig. 1(b) and (c), respectively. Unlike pure PPy films, which are brittle and mechanically less stable, the PPy/CS hybrid film is flexible and easily processable. As shown in Fig. 1(d), the hybrid film can be easily twisted and bent.
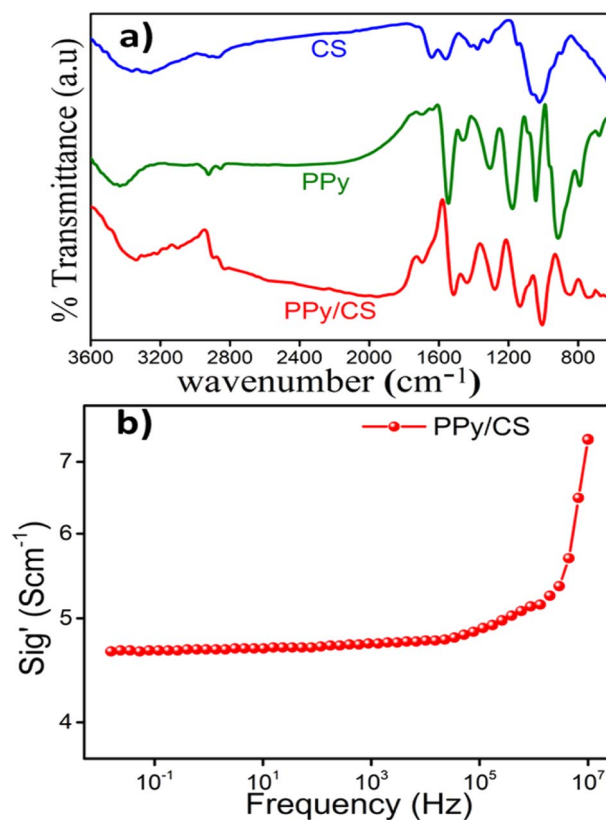

Fig. 2 (a) FTIR spectra of CS, PPy and the PPy/CS hybrid film. (b) Log–log plot of the frequency dependence of the ac conductivity of the PPy/CS hybrid film.

General characterization

Fig. 2(a) shows the FTIR spectra of the CS film, PPy and PPy/CS hybrid film. Characteristic peaks corresponding to both PPy and chitosan are shown for the hybrid film with slight modifications due to the existence of interactions between the components. Since the FTIR spectrum of the hybrid film was recorded using ATR technology, the major absorptions originate from the surface of the film and therefore correspond to PPy. The broad band at 3330 cm^{-1} in the FTIR spectrum of the hybrid film is attributed to the overlapping of the N–H stretch of pyrrole and O–H stretch of chitosan. As a consequence of the intermolecular hydrogen bonding interaction of the N–H group of PPy with the C=O group of CS, the C=O stretching vibration of the hybrid film is shifted to 1679 cm^{-1} from 1642 cm^{-1} of pristine chitosan. The peaks at 1516 and 1434 cm^{-1} are ascribed to the characteristic asymmetric and symmetric ring stretching vibrations of PPy, respectively.[44] The peaks at 1136 and 1008 cm^{-1} are attributed to the C–N stretching vibration and N–H in-plane deformation vibration, respectively, which indicates the doping state of PPy.

The frequency-dependent electrical conductivity of the PPy/CS hybrid film measured using broadband dielectric spectroscopy was found to be 4.55 S cm^{-1} (Fig. 2(b)). The hybrid film shows good electrical characteristics even though the main constituent of the hybrid film is insulating chitosan. This suggests the homogeneous distribution of PPy on the surface and inside of the CS film. Although the conductivity appears to be lower than that of pure PPy (2.4×10^2 S cm^{-1}), it is high enough in the hybrid system to show reaction driven sensing properties.

FESEM micrographs of the CS film and PPy/CS hybrid film are shown in Fig. 3(a)–(c). The chitosan film exhibits a smooth and homogenous surface morphology without any imperfections (Fig. 3(a)). Compared with the CS film, after *in situ* chemical polymerization with pyrrole, the PPy/CS hybrid film (Fig. 3(b) and (c)) possesses an agglomerated granular morphology composed of an aggregation of particles with nanometer dimensions, providing sufficient porosity and surface area to enable the diffusion of counterions and solvents for efficient electrochemical reaction. Representative EDX spectra of both films are shown in Fig. 3(d) and (e) and show only the desired elements (C, N, O, and Cl) on the surface. The appearance of Cl in Fig. 3(e) is strong evidence for the doping of PPy with Cl$^-$ ions (counter ions) in the hybrid film, and no additional elements are observed in the spectrum. The EDX results support the polymerization of pyrrole at the surface of the CS film.

TGA was used to assess the thermal stability and degradation behavior of the PPy/CS hybrid film and the resultant thermogram is presented in Fig. 4(a). The hybrid film shows two stages of mass loss. The first stage is related to the loss of water absorbed by the film during the chemical polymerization process in an aqueous medium. The second stage corresponds to the loss of dopants and polymer degradation and begins at approximately 170 °C. The film exhibits a degradation temperature of 196 °C, which is high enough for its biological applications. After the end of the process at 650 °C, the residual weight of the hybrid film is 40%. The mechanical properties of the PPy/CS hybrid film were evaluated from the experimental stress–strain curve (Fig. 4(b)). The tensile strength (maximum stress), Young's modulus and percentage elongation (maximum strain) of the hybrid film were found to be 5.7743 MPa, 2.314 MPa and 3.2076%, respectively. Free-standing PPy films generated by electrochemical methods are highly brittle and fragile, and thus have low mechanical strength, which limits their applicability as free-standing electrode materials. The
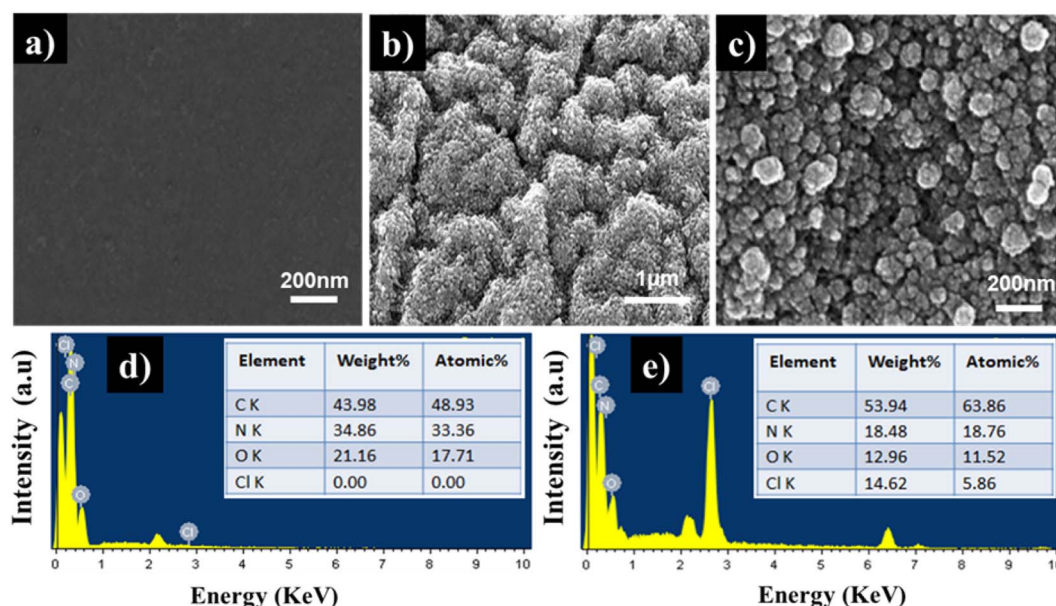

Fig. 3 SEM images of (a) pure CS, (b) the PPy/CS hybrid film at high resolution, and (c) the PPy/CS hybrid film at low resolution. EDX spectra of (d) pure CS, (e) the PPy/CS hybrid film.
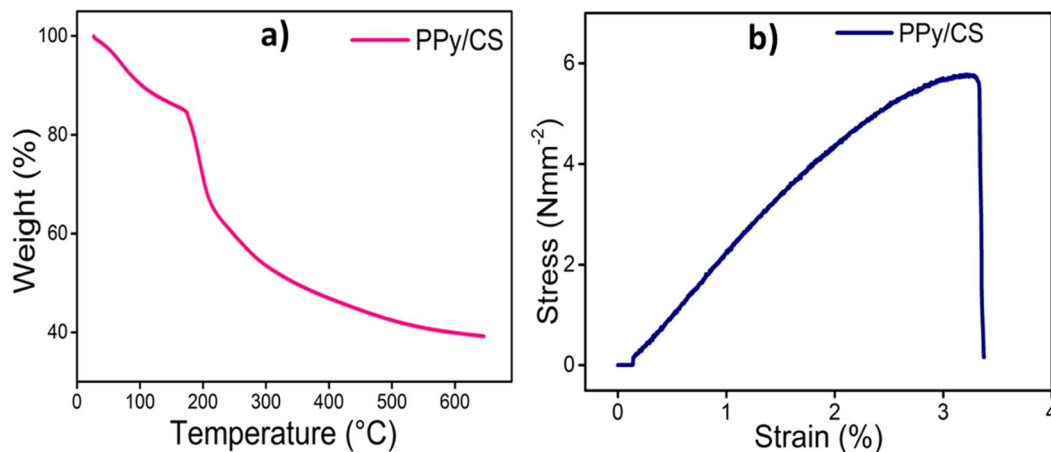
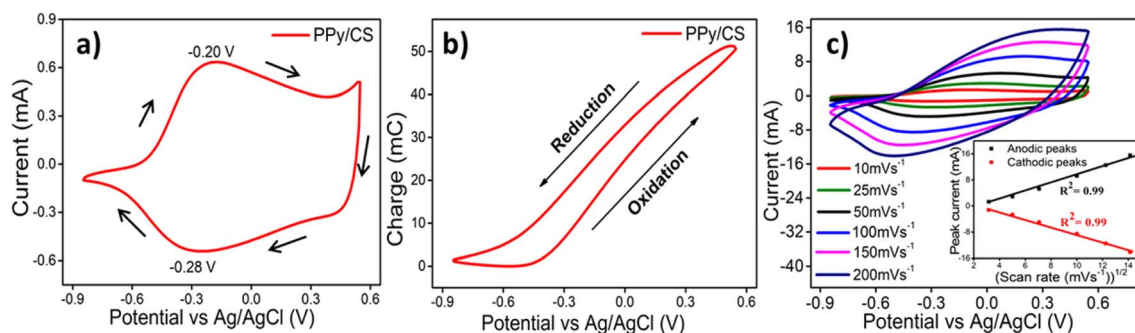Fig. 4 (a) TGA thermogram and (b) stress–strain curve of the PPy/CS hybrid film.

Fig. 5 (a) Stationary voltammetric response of the PPy/CS hybrid film at a scan rate of 10 mV s^{-1} in 1 M NaCl aqueous solution when it is subjected to potential cycles between −0.85 and 0.55 V vs. an Ag/AgCl electrode, (b) coulovoltammograms attained by integrating the CV of scan rate 10 mV s^{-1} presented in (a) in 1 M NaCl aqueous solution, (c) stationary voltammetric responses at different scan rates (the inset figure shows the variation of the peak current obtained from the voltammograms as a function of the square root of the scan rate).

fabricated hybrid film has good mechanical properties, making it a promising candidate to be used as an electrode material for electrochemical applications and devices.

Voltammetric response

The hybrid film was subjected to voltammetric cycles at room temperature in 1 M NaCl solution between −0.85 and 0.55 V at a scan rate of 10 mV s^{-1} in a three-electrode cell assembly. After 10 consecutive cycles, the voltammograms overlapped because previous structural memory had been erased from the material, and the eleventh voltammetric response is shown in Fig. 5(a). The obtained CV curve shows a pair of redox peaks due to faradaic redox behavior, and the resemblance of the oxidation/reduction peak with that of pure PPy certified that the electroactivity of the hybrid film is imparted by PPy. The voltammogram shows a broad anodic maximum corresponding to PPy oxidation at −0.20 V and a broad cathodic maximum corresponding to PPy reduction at −0.28 V. As the scan rate is low, the oxidation and reduction potentials are applied after large time intervals and thus promote deeper conformational changes. Hence an increased amount of free volume is generated/destroyed to insert/eject an increased number of

counterions and solvent molecules, with the consumption of a large amount of redox charge. Thus we get deeper oxidation/reduction states at low scan rates.

Only the reversible redox reaction that occurs in the hybrid film is identified from the voltammetric responses. The possible presence of irreversible reactions like hydrogen evolution is better visualized by the integration of the voltammograms into coulovoltammograms.[45,46] Fig. 5(b) shows the coulovoltammograms (QV, consumed charge vs. applied potential) obtained by integrating the CV presented in Fig. 5(a). The QV of the hybrid film is composed of a closed loop in the studied potential interval revealing that only reversible oxidation/reduction reactions take place in the film and the charge of the oxidation process is equal to that of the reduction process. If there is no such balance, the QV loops are either open or give a closed loop along with an open fraction.[46,47] The minimum of the QV is considered the zero-charge reference and the difference between the closed QV loop maximum and minimum points defines the charge (51.29 mC) consumed during the reversible PPy oxidation–reduction reaction.

Fig. 5(c) represents the CV loops of the hybrid film recorded at various scan rates ranging from 5 mV s^{-1} to 200 mV s^{-1}. Due to the rapid response of the oxidation/reduction to the current

changes, the current of the anodic and cathodic peaks increases dramatically with the increase of the scan rate. At higher scan rates, the intensity of redox peaks is weakened due to the fact that there is less time for the electrolyte to interact with the electrode in the fast electrochemical processes. The variation of the cathodic/anodic peak current *versus* the square root of the scan rate of the hybrid film is shown in the inset of Fig. 5(c), exhibiting a smooth linear relationship with a higher correlation coefficient ($R^2 = 0.99$) up to 200 mV s^{-1}, as expected for a diffusion controlled electrochemical process.

EIS studies were performed to investigate the fundamental electrochemical behavior of the hybrid film and the Nyquist plot is shown in Fig. 6. The Nyquist plot is composed of two well-separated patterns: a semicircle in the high-frequency part followed by an inclined line in the low-frequency part. The x-intercept of the impedance curve in the high-frequency region (2.45 Ω) gives the equivalent series resistance (ESR), which is the sum of the solution resistance, intrinsic resistance and contact resistance of the electrode to the current collector. The low value of the ESR is ascribed to the high hydrophilicity of the hybrid film and thus enables the penetration of counterions and solvent to the PPy chain through the swollen chitosan matrix and facilitates the electrochemical reactions. The semicircle at the high-frequency region depicts the charge transfer process and its diameter indicates the charge transfer resistance resulting from faradaic reactions and double-layer capacitance at the interface of the electrode and electrolytic solution. The inclined line in the low frequency region is attributed to the diffusion-limited ion transport at the electrode–electrolyte interface and its slope represents the diffusion resistance. The straight line leans towards the imaginary axis due to the porous nature of the electrode and its relatively large slope indicates more diffusion of the ions. To further understand the behavior of the fabricated hybrid film, an equivalent circuit model (inset of Fig. 6) is proposed to fit the Nyquist diagram by Zman software. In the circuit diagram, R_s (2.45 Ω), R_{ct} (31.5 Ω) and R_d (3.91 Ω) signify the solution resistance, charge transfer resistance and
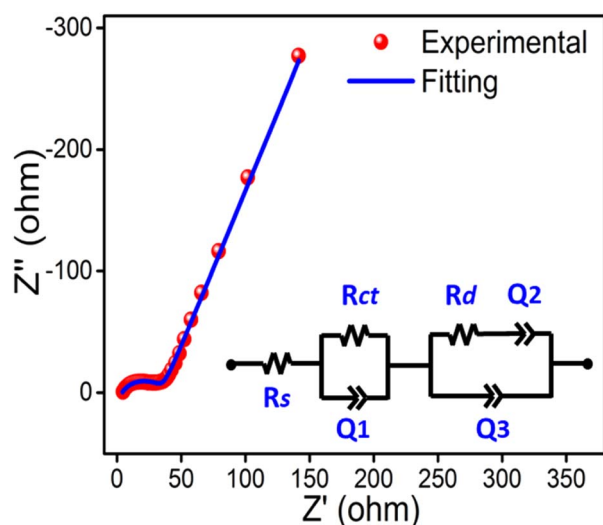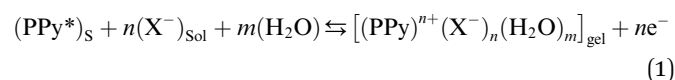
diffusion resistance, respectively. Q1, Q2 and Q3 are used to express the constant phase elements. These results suggest that the PPy/CS hybrid film should be considered a good electrode material and is advantageous for electrochemical applications such as reaction driven sensing.

Influence of temperature on the voltammetric responses

Fig. 7(a) displays the stationary voltammetric response of the PPy/Cs hybrid film at different temperatures (ranging from 10 °C to 50 °C) under constant chemical (electrolyte concentration), physical (potential limit and scan rate) and mechanical (pressure) conditions. The temperature of the electrolyte (1 M NaCl) first increases from 10 °C to 50 °C and then decreases from 50 °C to 10 °C. The voltammetric responses illustrate the increase of both the anodic and cathodic peak currents with the increase of temperature and then the decrease with the decrease of temperature. From Fig. 7(a), it is evident that similar voltammetric responses are attained for experiments at the same temperatures under the same working energetic conditions, corroborating the reproducibility of the redox reaction in the hybrid film. The voltammetric response of the control solution (1 M NaCl aqueous solution at 25 °C) was recorded between consecutive experiments at two different temperatures (Fig. 7(b)). The overlapping of the CVs in Fig. 7(b) indicates that the electrochemical activity of the hybrid film remained constant during the experiments.

The stationary QV responses obtained by integrating the CVs from Fig. 7(a) are presented in Fig. 8(a). It is observed that all the QVs are composed of a closed loop in the studied potential interval related to the PPy reversible oxidation/reduction reaction and guaranteeing the absence of any simultaneous irreversible reaction such as solvent electrolysis taking place in the studied potential interval. The difference between the closed QV loop maximum and minimum points defines the charge consumed during the reversible PPy oxidation–reduction reaction at different experimental temperatures. As the experimental temperature increases, the redox charge consumed during the reversible reactions driving the conformational movements of the reactive polymeric chain increases under the same chemical, physical and mechanical energetic conditions. Thus we get deeper oxidation/reduction states at higher temperatures.[48] It is notable that a similar redox charge is obtained for experiments of the same temperatures under the same working energetic conditions. Fig. 8(b) displays the stationary QV responses of the voltammetric control obtained by integrating the CVs from Fig. 7(b). The fact that these QVs can be superimposed confirms the reproducibility of the electroactivity of the hybrid film.

The electrochemical reversible reaction driving the exchange of anions by a p-doping/p-dedoping process (oxidation/reduction) using the PPy/CS hybrid film as the working electrode in a liquid electrolyte can be represented in its simplest form as,
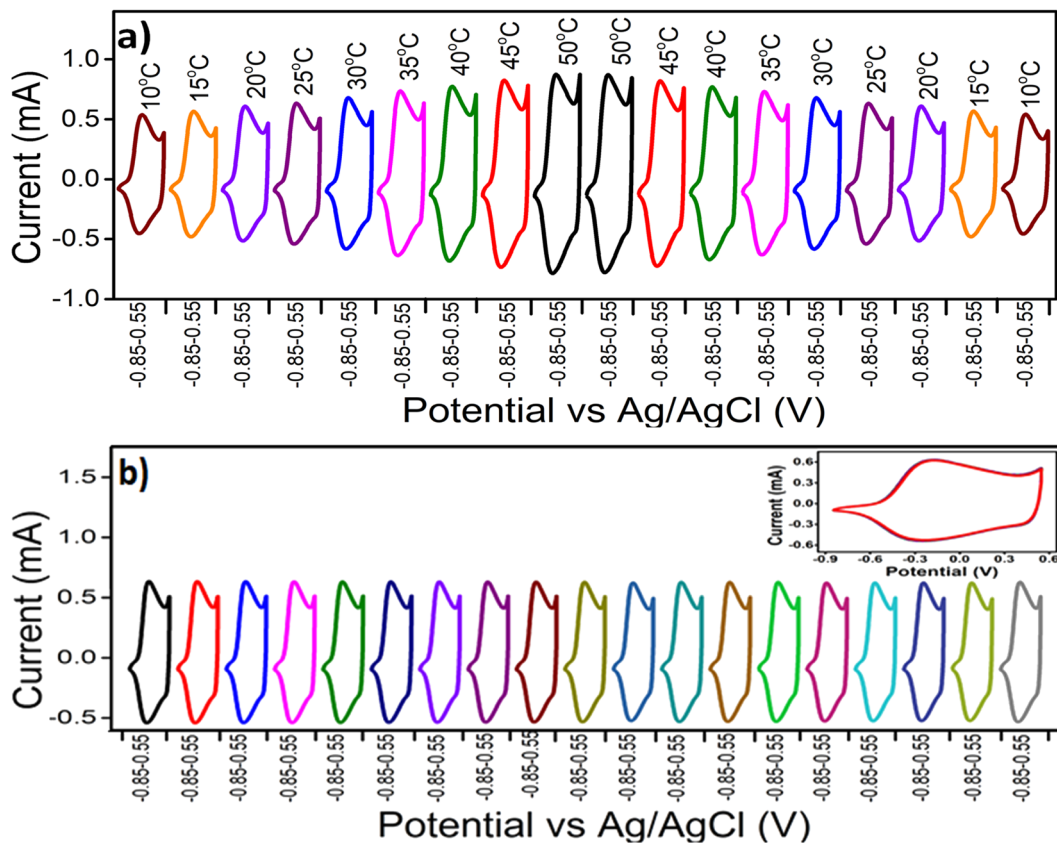

Fig. 6 Nyquist plot of the PPy/CS hybrid film.

$$(\text{PPy*})_S + n(\text{X}^-)_{\text{Sol}} + m(\text{H}_2\text{O}) \leftrightarrows \left[(\text{PPy})^{n+}(\text{X}^-)_n(\text{H}_2\text{O})_m \right]_{\text{gel}} + n\text{e}^-$$

$$(1)$$

Fig. 7 (a) Stationary voltammetric responses obtained after three consecutive voltammograms at different temperatures cycled between −0.85 and 0.55 V at 10 mV s^{-1} in 1 M NaCl aqueous solution, (b) voltammetric responses of the control solution (1 M NaCl aqueous solution at 25 °C) obtained after each experiment with the same potential interval and scan rate (the inset shows the superimposed control CVs).

where PPy* denotes the active centers on any polymer chain taking part in the PPy/CS hybrid film (indicated by the sub-index S) where positive charges are generated by oxidation, X$^-$ is the monovalent anion exchanged with the electrolyte solution (indicated by the sub-index Sol) to balance the chain positive charge, n is the number of anions exchanged for charge balance or the number of electrons removed per polymer chain, H$_2$O molecules are exchanged to retain the osmotic balance and m is the number of exchanged solvent molecules. The forward process is the oxidation process during which free volume is generated in the polymer film by the cooperative actuation of the constitutive polymeric chains. Thus anions and solvent molecules enter into the polymer chain, the polymer swells and the composition changes from [PPy*] to the $[(PPy)_n^+(X^-)_n(H_2O)_m]$ gel. This gel formation occurs not through a single step but through n consecutive steps (energetic conformational states) of one electron extraction per step related to the first, second..., nth ionization potentials of the polymer chain. The extraction of each electron results in a little conformational movement of the chain. The consecutive electronic extractions result in large conformational movements (cooperative actuation) of the chain supported by strong coulombic repulsion between the emerging polarons and attractive forces between the polarons and counterions, and polarons and water. The continuous variation of the composition of the polymer under faradaic control through

continuous extraction/insertion of electrons is responsible for the composition dependent properties of the conducting polymers. During reduction, electrons are inserted and the polymer shrinks by cooperative actuation with the expulsion of anions and solvent towards the solution. That is, the reversible electrochemical reactions of the conducting polymer control the conformational and structural changes and act as an electrochemical molecular (polymeric) machine. As the electron extractions occur through n energetic conformational states, each PPy chain acts as a multistep macromolecular polymeric motor.[49] The number of ions and solvent molecules exchanged and the volume variation must depend on the number of electrons involved (charge) in the electrochemical reaction (Faraday's law).

Sensing working thermal conditions

Working at a low temperature means that the reaction occurs under the demands of low available thermal energy and allows partial conformational movements of the reactant polymeric chains. The partial conformational relaxation of the polymeric chains generates a low amount of free volume in which to insert the counterions and the solvent molecules with concomitant consumption of low oxidation charge.[50] Due to the partial exchange of counterions and solvent molecules, the polymer chains undergo partial oxidation/reduction at low
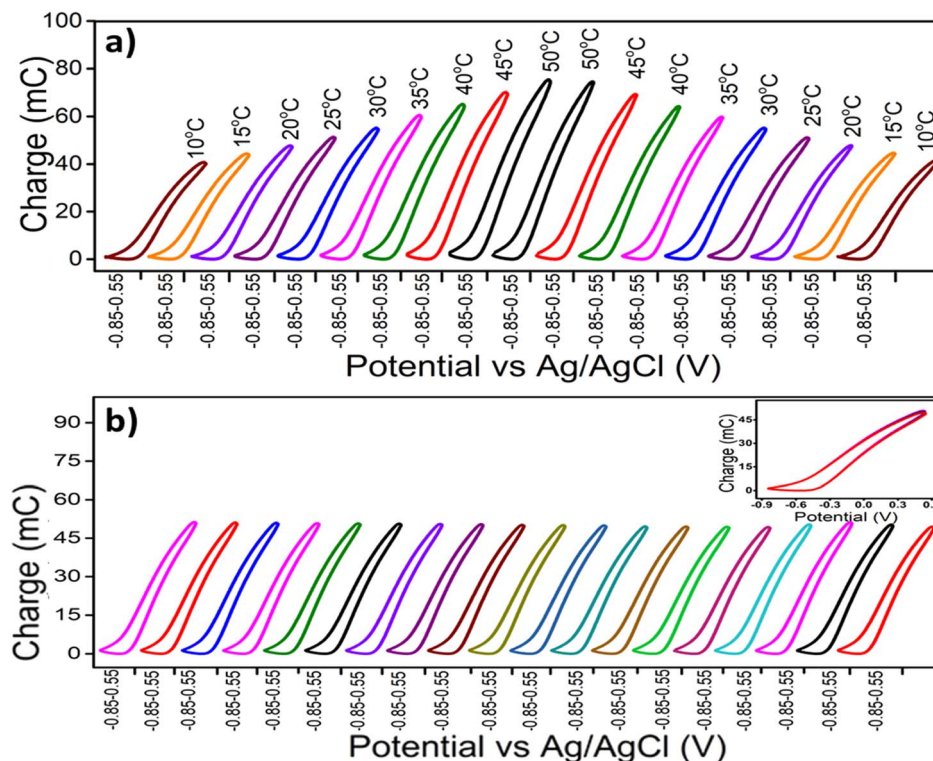
Fig. 8 (a) Stationary coulovoltammograms obtained by the integration of the CVs presented in Fig. 7(a) at different experimental temperatures, (b) control coulovoltammograms obtained by integration of the control voltammograms presented in Fig. 7(b) (inset shows the superimposed control QVs).

temperatures.[51,52] As the experimental temperature increases, the increased available thermal energy allows faster and longer conformational movements of the polymeric chains, and produces/destroys increasing amounts of free volume to allow the entrance/ejection of increasing numbers of counterions and solvent molecules with the consumption of increasing redox charge as illustrated in Fig. 9. Thus, under the same chemical, mechanical and electrical conditions, we get deeper oxidation/reduction states at higher temperatures. The number of counterions and solvent molecules entering/ejected during reaction (1) is controlled by the redox charge. From Fig. 8(a), it is evident that as the temperature increases, the redox charge consumed by the reversible electrochemical reaction driving reversible conformational movements that give molecular motors in solution increases. Thus for any chemical or biochemical reaction based on the cooperative actuation of the constitutive polymer chains, the extension of reaction varies, at any instant, as a function of the temperature and temperature variations. That is, the redox charge acts as a self-sensor of the ambient thermal conditions of the reaction similar to natural muscle. Translated to molecular motors from natural muscle, higher redox charges are consumed by the muscular reactions occurring at higher temperatures.

Theoretical description of temperature sensing

The obtained results confirm that both the forward and backward reaction of reaction (1) driving the conformational and structural changes of the constitutive polymeric chains sense the experimental temperature. From a theoretical basis, the empirical kinetics of the forward reaction (1) can be represented as:

$$R = k[\text{PPy*}]^a[\text{X}^-]^b \tag{2}$$

where R is the rate of the reaction, k is the rate constant, $[\text{PPy*}]$ is the concentration of active centers of the polymer chains, $[\text{X}^-]$ is the concentration of counterions (here, Cl$^-$ ions), and the super-indexes a and b are the reaction orders concerning the concentration of active centers of the polymer chains and counterions in the solution. During the oxidation/reduction reactions, the volume of the hybrid film changes. Thus the rate of the reaction can be expressed in terms of the specific concentration of active centers as:

$$r = \frac{R}{m} = \frac{k}{m}[\text{PPy*}]^a[\text{X}^-]^b \tag{3}$$

where m is the unit mass of the dry material reacting inside the electrolyte during reaction (1). According to the Arrhenius equation, the temperature dependence of the reaction rate can be expressed:[53]

$$k = A\mathrm{e}^{-E_a/RT} \tag{4}$$

where A is the pre-exponential factor, E_a is the activation energy of the electrochemical reaction, R is the universal gas constant and T is the working absolute temperature.
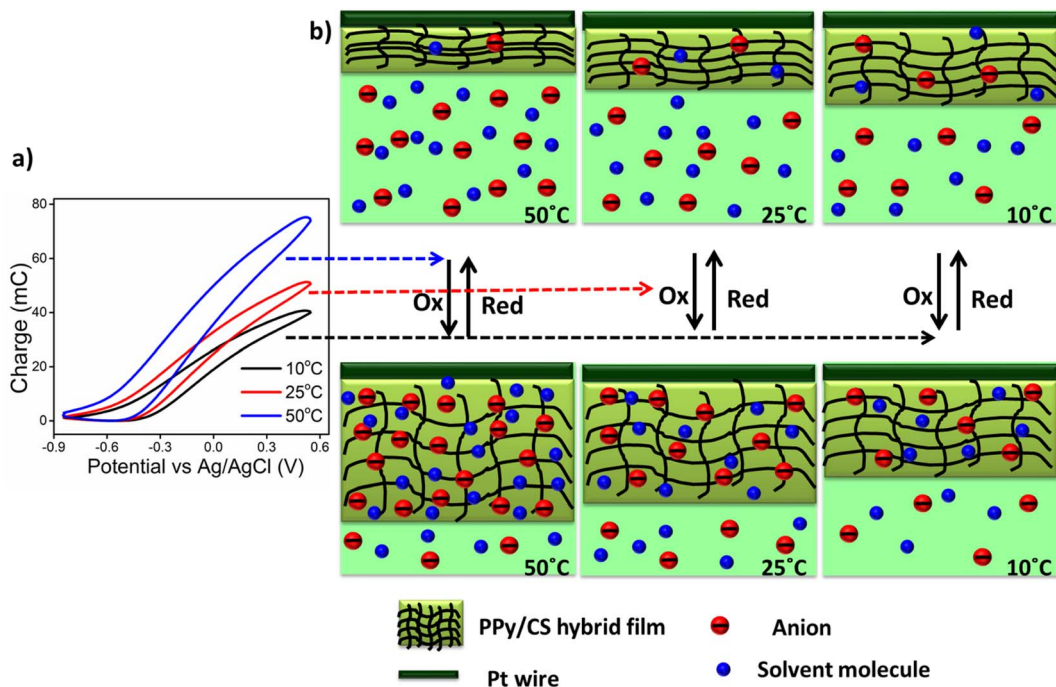
Fig. 9 (a) Coulovoltammetric responses showing the redox charges at 10 °C, 25 °C and 50 °C, (b) schematic representation of the extension of the structural changes (swelling/shrinking) by the reversible redox reaction of the PPy/CS hybrid film at 10 °C, 25 °C and 50 °C in 1 M NaCl aqueous solution under similar experimental conditions, where Ox means oxidation and Red means reduction.

According to the Faraday law, the variation of the concentration of active centers, [PPy*], in the hybrid film can be expressed in terms of the reaction charge involved (Q) as:

$$-\Delta[\text{PPy*}] = \frac{Q}{mzF} = \frac{q}{zF} \tag{5}$$

where z is the valence of the active center (taken as 1 in this case), F is the Faraday constant ($F = 96\ 485$ C mol^{-1}) and q is the specific charge ($q = Q/m$). The reaction rate can also be defined in terms of the variation of the specific concentration of active centers [PPy*] in the hybrid film per unit of time as:

$$r = -\frac{\partial[\text{PPy*}]}{\partial t} = -\frac{\partial}{\partial t}\frac{q}{F} = -\frac{1}{F}\frac{\partial q}{\partial t} \tag{6}$$

The average rate of the reaction in terms of the consumed coulovoltammetric charge (Q) and the time required to complete a potential scan ($\Delta E/v$) can be defined as:

$$\bar{r} = -\frac{\Delta[\text{PPy*}]}{\Delta t} = \frac{q}{Ft} = \frac{qv}{F\Delta E} \tag{7}$$

From eqn (3)–(7) the rate of reaction can be written as:

$$\frac{qv}{F\Delta E} = \frac{A\ \mathrm{e}^{-E_a/RT}}{m}[\text{PPy*}]^a[\text{X}^-]^b = \frac{A\ \mathrm{e}^{-E_a/RT}}{m}\left(\frac{q}{F}\right)^a[\text{X}^-]^b \tag{8}$$

The relationship between the consumed charge during the electrochemical reaction and the experimental temperature is obtained by rearranging eqn (8) as:

$$q^{1-a} = \frac{F^{1-a}\Delta E[\text{X}^-]^b A}{mv}\ \mathrm{e}^{-E_a/RT} \tag{9}$$

The constant terms in eqn (9) are considered as a new constant k' $\left[k' = \dfrac{F^{1-a}\Delta E[\text{X}^-]^b A}{mv}\right]$, then:

$$q^{1-a} = k'\mathrm{e}^{-E_a/RT} \tag{10}$$

Taking logarithms on both sides, we get a semilogarithmic relationship between the redox charge consumed during the reaction (at constant chemical, physical and mechanical conditions) and the experimental temperature:

$$(1-a)\ln q = \ln k' - \frac{E_a}{RT} \tag{11}$$

$$\ln q = c + d\frac{1}{T} \tag{12}$$

Eqn (12) represents a straight line equation with slope c and intercept d given by eqn (13) and (14), respectively:

$$c = \frac{\ln k'}{1-a} \tag{13}$$

$$d = \frac{E_a}{(1-a)R} \tag{14}$$

Eqn (12) describes how the redox charge or reaction extension during the potentiodynamic conditions responds to the

experimental thermal conditions. The redox charge defined by the coulovoltammetric charge varies as a semilogarithmic function of the inverse of the temperature. In other words, the electrochemical reaction of the hybrid film senses the experimental temperature.

During any potentiodynamic experiment, the average energy (U) consumed by reaction (1) at a constant potential E is:

$$U = EQ \tag{15}$$

From this equation, it is clear that, at higher temperatures, higher reaction energies are achieved due to the consumption of higher charges.

Fig. 10 displays the semilogarithmic variation of the redox charge or reaction extension of the reaction with the inverse of the temperature for both increasing and subsequent decreasing temperatures. By varying the temperature and keeping constant the values for the other experimental variables, a good agreement was achieved between the redox charges of experiments with the same temperatures. The experimental results are in good agreement with the sensing equation (eqn (12)). The slope of the linear dependency gives the thermal sensitivity of the sensor. Thus we can summarize that the electrochemical reactions of reactive PPy/CS hybrid films are sensors of the available thermal energy (temperature) of the reaction media.

The influence of the experimental temperature on the CV responses was analysed after 500 cycles of CV at a scan rate of 100 mV s^{-1} in 1 M NaCl aqueous solution at room temperature. After 500 CV cycles, the CV slightly deviates from the first cycle and a slight reduction in the redox charge occurs. However, the hybrid film retained about 96% of its sensitivity after 500 cycles (Fig. 10) suggesting excellent performance of the hybrid film as a temperature sensor. The retained sensitivity also suggests the reproducibility of the temperature sensing capability of the hybrid film.
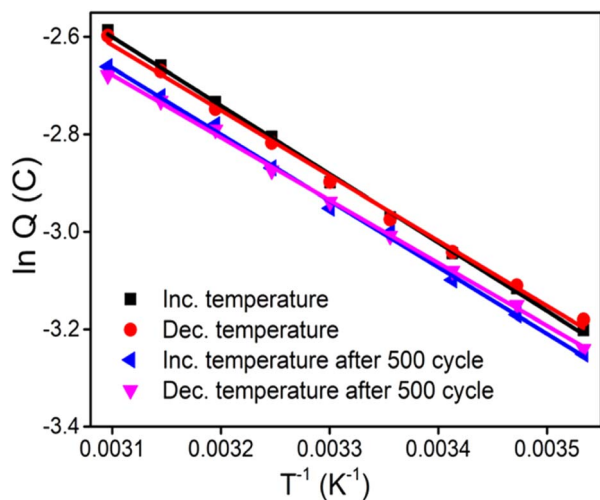

Fig. 10 Semilogarithmic variation of the electrical charge consumed by the reversible redox reactions of the hybrid film with the inverse of the temperature.

Biological perspectives

The rate of the reaction driving the cooperative conformational movements of the molecular motors constituting the sarcomere of natural muscle increases when the body temperature rises (as described by the Arrhenius relationship). Fig. 8(a) confirms that the redox charge (reaction extension or amplitude of the electrochemical reaction) increases with increasing temperature when the reaction is carried out under the same working energetic (physical, chemical and mechanical) conditions. Translated to the muscles of ectothermic beings, under the same brain order or the same energetic conditions, when the body temperature falls, the muscles respond by decreasing the amplitude of the muscle movement (extension) generated by the same electrical pulse. That is, the muscular reactions occur in a faster and easier way (or show higher temperature-based efficiency) when the ectothermic animal is heated by exposure to sunlight or a thermal source. The experimental results could provide some quantitative explanation for the muscle-powered movements of ectothermic beings, which respond to thermal energy from the environment. Fig. 10 implies a lower consumption of reaction energy occurs at higher temperatures when the muscular reaction is carried out with constant mechanical energy (running, walking, stomach digestion and so on). In other words, the energy consumed (or the effort undertaken) by the muscle has to be increased to produce the same muscular action (reaction extension) at lower temperatures. Natural muscles are electro-chemo-mechanical and thermo-mechanical transducers, respond to the reaction energy under various thermal conditions and send sensing signals regarding the working thermal (chemical and physical) conditions generated at the muscle/dendrite interface to the brain through sensory neurons.

Conclusions

A polypyrrole/chitosan hybrid film capable of sensing working thermal conditions was fabricated through *in situ* chemical polymerization of pyrrole and investigated potentiodynamically at different temperatures. Polypyrrole is responsible for the good electronic conductivity and excellent electroactivity of the hybrid film and chitosan serves as an insulating matrix. SEM analysis showed that after *in situ* chemical polymerization with pyrrole, the hybrid film possesses an agglomerated granular morphology of PPy with sufficient porosity and surface area for it to allow efficient diffusion of ions and solvent and therefore, improve the electrochemical reactions. The hybrid film was electrochemically characterized in an aqueous solution of NaCl using cyclic voltammetry and the polymer chains acted as a multistep electrochemical molecular sensor. Under potentiodynamic conditions, the higher thermal energy available at higher temperatures stimulates deeper conformational movements due to the cooperative actuation of the constitutive polymeric chains, and deeper oxidation/reduction states due to increased consumed charge. The closed coulovoltammetric responses of the hybrid film confirm the reversible nature of the polypyrrole redox reactions and reveal the absence of

simultaneous irreversible reactions taking place in the studied potential window. The reaction extension or the consumed charge obtained from the closed coulovoltammetric loops responds to, adapts to, or is a sensor of the working thermal conditions. This self-sensing property allows one to suggest that any device/motor constructed using these materials and driven by the conformational movements of the macromolecular reactants will sense the thermal energetic conditions while working. The hybrid film is considered here as a model material that replicates the reactions taking place in the muscle sarcomere. The results provide a possible quantitative description of the muscular reactions of ectothermic (cold-blooded) animals at different temperatures.

Author contributions

Y. A. Ismail: conceptualization, supervision, formal analysis, methodology, writing – review and editing the draft; A. K. Shabeeba: investigation, formal analysis, methodology, validation, writing – original draft; M. P. Sidheekha: validation, formal analysis, writing – review and editing; L. Rajan: validation, formal analysis, writing – review and editing.

Conflicts of interest

There are no conflicts of interest to declare.

Acknowledgements

References

1 T. F. Otero, *Phys. Chem. Chem. Phys.*, 2017, **19**, 1718–1730.
2 A. F. Huxley and R. M. Simmons, *Nature*, 1971, **233**, 533–538.
3 T. F. Otero, *Polym. Rev.*, 2013, **53**, 311–351.
4 J. Gillooly, E. L. Charnov, G. B. West, V. M. Savage and J. H. Brown, *Nature*, 2002, **417**, 70–73.
5 R. B. Huey and J. G. Kingsolver, *Trends Ecol. Evol.*, 1989, **4**, 131–135.
6 T. L. Wilson and R. B. Reeves, *Respir. Physiol.*, 1976, **28**, 29–47.
7 S. Beaumont and T. Otero, *ChemElectroChem*, 2017, **10**, 3091–3099.
8 T. F. Otero and J. G. Martinez, *J. Mater. Chem. B*, 2013, **1**, 26–38.
9 T. F. Otero, *J. Mater. Chem. B*, 2013, **1**, 3754–3767.
10 T. F. Otero and J. G. Martinez, *Sens. Actuators, B*, 2014, **199**, 27–30.
11 T. F. Otero and S. Beaumont, *Sens. Actuators, B*, 2017, **253**, 958–966.
12 T. F. Otero and M. J. Ariza, *J. Phys. Chem. B*, 2003, **107**, 13954–13961.
13 T. F. Otero, *J. Mater. Chem.*, 2009, **19**, 681–689.
14 M. P. Sidheekha, K. Nufaira, A. Shabeeba, L. Rajan and Y. A. Ismail, *Mater. Today: Proc.*, 2022, **51**, 2286–2292.
15 T. F. Otero and J. G. Martinez, *Prog. Polym. Sci.*, 2015, **44**, 62–78.
16 T. F. Otero and S. Beaumont, *Sens. Actuators, B*, 2018, **263**, 493–501.
17 J. G. Martinez and T. F. Otero, *Sens. Actuators, B*, 2014, **195**, 365–372.
18 T. F. Otero and S. Beaumont, *Electrochim. Acta*, 2017, **258**, 1293–1303.
19 T. F. Otero, J. J. Sanchez and J. G. Martinez, *J. Phys. Chem. B*, 2012, **116**, 5279–5290.
20 D. E. Rassier, *Am. J. Physiol. Cell Physiol.*, 2017, **313**, C134–C145.
21 K. Namsheer and C. S. Rout, *RSC Adv.*, 2021, **11**, 5659–5697.
22 X. Fan, Z. Yang and N. He, *RSC Adv.*, 2015, **5**, 15096–15102.
23 J. Gao, A. Heeger, J. Lee and C. Kim, *Synth. Met.*, 1996, **82**, 221–223.
24 P. Novák, K. Müller, K. Santhanam and O. Haas, *Chem. Rev.*, 1997, **97**, 207–282.
25 R. T. Richardson, A. K. Wise, B. C. Thompson, B. O. Flynn, P. J. Atkinson, N. J. Fretwell, J. B. Fallon, G. G. Wallace, R. K. Shepherd and G. M. Clark, *Biomaterials*, 2009, **30**, 2614–2624.
26 F. G. Córdova, Y. A. Ismail, J. G. Martinez, A. S. Al Harrasi and T. F. Otero, *International Society for Optics and Photonics*, 2013, vol. 8687, pp. 29–43.
27 C. Wang, W. Zheng, Z. Yue, C. O. Too and G. G. Wallace, *Adv. Mater.*, 2011, **23**, 3580–3584.
28 Y. A. Ismail, J. G. Martínez, A. S. Al Harrasi, S. J. Kim and T. F. Otero, *Electroactive Polymer Actuators and Devices (EAPAD)*, 2011, vol. 7976, pp. 450–461.
29 Y. A. Ismail, J. G. Martinez and T. F. Otero, *J. Electroanal. Chem.*, 2014, **719**, 47–53.
30 E. Smela, *Adv. Mater.*, 2003, **15**, 481–494.
31 A. Ben Slimane, M. M. Chehimi and M.-J. Vaulay, *Colloid Polym. Sci.*, 2004, **282**, 314–323.
32 Y. A. Ismail, A. Shabeeba, M. P. Sidheekha and L. Rajan, *Actuators: Fundamentals, Principles, Materials and Applications*, 2020, pp. 211–252.
33 A. N. Raja, *Int. J. Biol. Macromol.*, 2020, **164**, 4231–4244.
34 A. Karrat and A. Amine, *Arabian J. Chem. Environ. Res.*, 2020, **7**, 66–93.
35 F. Croisier and C. Jérôme, *Eur. Polym. J.*, 2013, **49**, 780–792.
36 A. Shabeeba and Y. A. Ismail, *Mater. Res. Bull.*, 2022, **152**, 111817.
37 L. Rajan, M. P. Sidheekha, A. Shabeeba and Y. A. Ismail, *Mater. Chem. Front.*, 2022, **6**, 1706–1718.
38 M. P. Sidheekha, L. Rajan and Y. A. Ismail, *Mater. Chem. Phys.*, 2022, **279**, 125769.
39 A. Shabeeba, M. M. Manikandan, M. P. Sidheekha, L. Rajan and Y. A. Ismail, *Mater. Today: Proc.*, 2022, **51**, 2293–2299.

40 M. P. Sidheekha, G. E. Rajendran, A. Shabeeba and Y. A. Ismail, *J. Mater. Res.*, 2021, **36**, 1914–1926.

41 R. Rajamany, S. Prakash and Y. A. Ismail, *Plast., Rubber Compos.*, 2022, **51**, 240–249.

42 Y. A. Ismail, J. G. Martínez, A. S. Al Harrasi, S. J. Kim and T. F. Otero, *Sens. Actuators, B*, 2011, **160**, 1180–1190.

43 A. Shabeeba, L. Rajan, M. P. Sidheekha, M. S. Thayyil and Y. A. Ismail, *J. Energy Storage*, 2022, **55**, 105724.

44 G. Ruhi, O. Modi and S. Dhawan, *Synth. Met.*, 2015, **200**, 24–39.

45 T. F. Otero, *Electrochim. Acta*, 2016, **212**, 440–457.

46 T. F. Otero, M. Alfaro, V. Martinez, M. A. Perez and J. G. Martinez, *Adv. Funct. Mater.*, 2013, **23**, 3929–3940.

47 T. F. Otero, J. Schumacher and V. H. Pascual, *RSC Adv.*, 2016, **6**, 68538–68544.

48 Y. A. Ismail, J. G. Martínez and T. F. Otero, *Electrochim. Acta*, 2014, **123**, 501–510.

49 L. Valero, J. G. Martinez and T. F. Otero, *J. Solid State Electrochem.*, 2015, **19**, 2683–2689.

50 T. Otero and H. Grande, *J. Electroanal. Chem.*, 1996, **414**, 171–176.

51 H. Grande and J. Rodríguez, *Synth. Met.*, 1997, **85**, 1077–1078.

52 T. Otero, H. Grande and J. Rodriguez, *J. Electroanal. Chem.*, 1995, **394**, 211–216.

53 T. F. Otero and S. Beaumont, *Electrochim. Acta*, 2017, **257**, 403–411.

© 2022 The Author(s). Published by the Royal Society of Chemistry